JTTEE5 14:530-535
DOI: 10.1361/105996305X76577
1059-9630/$19.00 © ASM International

Peer Reviewed

Photoresponse and Donor Concentration of Plasma-Sprayed TiO_2 and TiO_2-ZnO Electrodes

F.-X. Ye, A. Ohmori, and C.-J. Li

(Submitted October 4, 2004; in revised form December 28, 2004)

The photoelectrochemical characteristics of plasma-sprayed porous TiO_2, TiO_2-5%ZnO, and TiO_2-10%ZnO electrodes in 0.1 N NaOH solution were studied through a three-electrode cell system. The microstructure, morphology, and composition of the electrodes were analyzed using an electron probe surface roughness analyzer (ERA-8800FE), scanning electron microscopy, and x-ray diffraction. The results indicate that the sprayed electrodes have a porous microstructure, which is affected by the plasma spray parameters and composition of the powders. The TiO_2-ZnO electrodes consist of anatase TiO_2, rutile TiO_2, and $Zn_2Ti_3O_8$ phase. The photoresponse characteristics of the plasma-sprayed electrodes are comparable to those of single-crystal TiO_2, but the breakdown voltage is close to 0.5 V (versus that of a saturated calomel electrode). The short-circuit photocurrent density (J_{SC}) increases with a decrease of donor concentration, which was calculated according to the Gartner-Butler model. For the lowest donor concentration of a TiO_2-5%ZnO electrode sprayed under an arc current of 600 A, the short-circuit J_{SC} is approximately 0.4 mA/cm^2 higher than that of the TiO_2 electrodes under 30 mW/cm^2 xenon light irradiation. The J_{SC} increases linearly with light intensity.

Keywords electrode, photoelectrochemical characteristic, plasma spraying, TiO_2, ZnO

1. Introduction

Since professors Fujishima and Honda discovered the photoelectrolysis of water on TiO_2 electrodes in 1972, extensive studies have been performed to understand the fundamental principles and improve the electrode (cell) properties of TiO_2, such as light harvesting, light-converting components, photocurrent density (J_{SC}), open circuit voltage, fill factor, stability (Ref 1,2). Mostly due to its lower cost compared with single-crystalline TiO_2, polycrystalline n-TiO_2 has been mainly studied as a semiconductor electrode in photoelectrochemical cells (Ref 3). Many techniques can be implemented for the preparation of the photoelectrode, including wet chemical processing (e.g., sol-gel and screen printing), vapor-processing techniques (e.g., chemical vapor deposition [CVD], physical vapor deposition [PVD]), and thermal oxidation of Ti (Ref 4). However, the electrodes prepared by the above-mentioned methods have many defects; for example, the electrode adhesion strength of the substrate is generally very low, which results in an increase in the ohmic resistance and hence in a lower cell power.

To improve the J_{SC} of TiO_2 electrodes, one method is to obtain optimal electrical resistivity of the electrodes. It is reported that ZnO additive can change the electrical resistivity of TiO_2 due to the formation of defects and zinc titanate (Ref 5).

Thermal spraying is an economical and versatile fabrication process for producing large surface coatings with almost unlimited types of materials. The coating thickness, texture, and bonding strength can be controlled through, for instance, spray-processing parameters, powders, and the spray method (Ref 3). Furthermore, many experimental studies and modeling works clearly indicate a very significant entrapment of air (cold, low viscosity, dense, with almost null velocity) within the plasma jet (high temperature, high viscosity, low density, and high velocity) inducing a drastic cool-down of the jet, and consequently the molecular dissociation and ionization of O_2 and N_2 molecules and O and N atoms. Therefore, in the current study, TiO_2 and TiO_2-ZnO electrodes were prepared on a stainless steel substrate by plasma spraying. The microstructure and photoelectrochemical characteristics of the electrodes were analyzed with an electron probe surface roughness analyzer (ERA-8800FE, Elionix, Japan), a scanning electron microscope (SEM), x-ray diffraction (XRD), and a three-electrode cell system equipped with a quartz window.

2. Materials and Experimental Procedures

2.1 Materials

The variation of photoelectrochemical properties with grain size is associated with an increase in the specific area and a corresponding increase in the light harvesting. If the size of the feedstock powder is smaller than 10 μm, it is difficult to deposit a coating by thermal spraying due to the difficulties with injecting the particles into the spray jet for their low mass and momentum. Furthermore, it is difficult to feed these small particles with standard equipment. So, to avoid these difficulties, the primary particle diameter of TiO_2 was about 0.2 μm, and polyvinyl alco-

The original version of this paper was published as part of the DVS Proceedings: "Thermal Spray Solutions: Advances in Technology and Application," International Thermal Spray Conference, Osaka, Japan, 10-12 May 2004, CD-Rom, DVS-Verlag GmbH, Düsseldorf, Germany.

F.-X. Ye and **A. Ohmori,** Joining and Welding Research Institute, Osaka University, Osaka, 567-0047, Japan; and **C.-J. Li,** Welding Research Institute, School of Materials Science and Engineering, Xi'an Jiaotong University, Xi'an, Shaanxi, 710049, Peoples Republic of China. Contact e-mail: yefx@jwri.osaka-u.ac.jp.

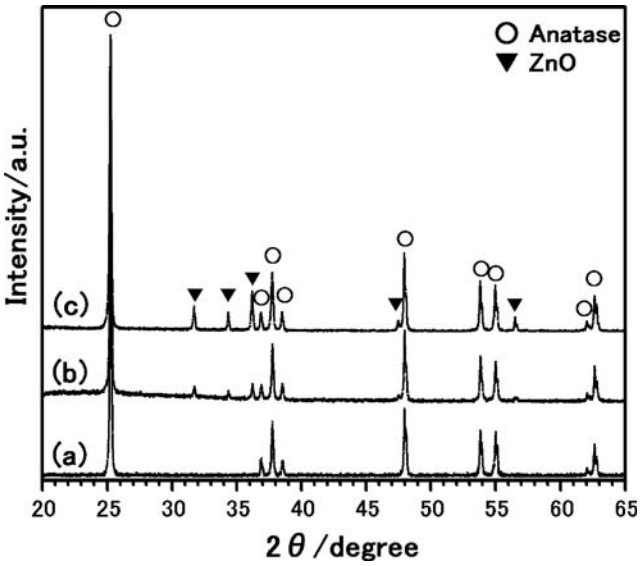

Fig. 1 XRD patterns of feedstock powders: (a) TiO_2; (b) TiO_2-5%ZnO; and (c) TiO_2-10%ZnO

hol was used as a binder for the thermal spray feedstock with particles having an average diameter of 33.7 μm. Because the photoelectrochemical property of anatase titanium dioxide is better than that of rutile TiO_2, anatase TiO_2 was used as feedstock powder. It is reported that ZnO can improve the photoelectrochemical properties of the TiO_2 electrode (Ref 5). Therefore, to investigate the influence of the ZnO additive, and based on data from the report of Yoon et al. (Ref 5), TiO_2-5%ZnO and TiO_2-10%ZnO powders were designed for this study. The average size of particles in the TiO_2-ZnO powder was also approximately 30 μm. XRD patterns of the feedstock powders are illustrated in Fig. 1. The substrate was stainless steel (JIS SUS316).

2.2 Plasma Spray Equipment

A Plasma Dyne system (Plasmadyne Mach1, Miller Thermal, MA) was used to spray TiO_2, TiO_2-5%ZnO, and TiO_2-10%ZnO electrodes. Argon was used as a primary plasma gas, and helium was used as the secondary gas. The spray parameters standard liter per minute (slpm) are listed in Table 1.

2.3 Analysis of the Feedstock Powders and Sprayed Electrodes

The electron probe surface roughness analyzer (ERA-8800FE) and the SEM were used to examine the structural characteristics of the feedstock powders and the sprayed electrodes. Their phase compositions were investigated by XRD using Cu-Kα radiation (λ = 1.5406 Å) with a graphite crystal monochromator (JDX3530, JEOL, Japan).

2.4 Photoelectrochemical Characteristics Evaluation Apparatus and Process

Voltammetry was performed in a three-electrode glass cell at room temperature, in which a commercial saturated calomel electrode (SCE) was used as the reference electrode and a platinum plate (30*30 mm) was used as the counter electrode. The

Table 1 Plasma spray conditions for a Plasma Dyne spray system

Conditions	Values
Argon primary gas flow, slpm	58
Helium gas flow, slpm	9
Arc current, A	400, 600, 800
Arc voltage, V	28~30
Spraying distance, mm	70
Feedstock rate, rpm	4
Anode type	2083-145
Cathode type	1083A-129

electrolyte was a 0.1 N NaOH solution and was deaerated by purging with Ar gas for 30 min before the experiments. The photocurrent against the potential at each sprayed electrode (working electrode) was measured using a scanning potentiostat and was recorded with a personal computer through an AD converter (NR-110, KEYENCE Corporation, Japan). The sweep speed of the potential was 2 mV/s in every experiment except in transient photocurrent measurement experiment. A 500 W xenon lamp was used as the light source, and the light intensity was measured with an ultraviolet radiometer (UVR-2, TOPCON, Tokyo, Japan) with a UD-40 detector.

3. Results and Discussion

3.1 Microstructure of the Sprayed TiO_2 and TiO_2-ZnO Electrodes

Figure 2 shows the typical microstructures of TiO_2, TiO_2-5%ZnO, and TiO_2-10%ZnO electrodes prepared by plasma spray under an arc current of 600 A. The sprayed electrodes are not very dense and contain many pores. The coating porosity increases with increasing amounts of ZnO. This may result from the volatilization of Zn during the deposition process, as clearly shown in Fig. 3, where the spherical pores remain.

As shown in Fig. 4, the TiO_2-5%ZnO electrode density increases with an increase of the arc current. The feedstock powder is very likely more melted under the higher arc current.

The typical XRD pattern of plasma-sprayed TiO_2-5%ZnO electrodes is illustrated in Fig. 5. The electrode consists of anatase TiO_2, rutile TiO_2, and $Zn_2Ti_3O_8$ phases. Despite its relative instability, the formation of $Zn_2Ti_3O_8$ phase rather than the Zn_2TiO_4 phase is rational due to the similarity in structure between anatase and $Zn_2Ti_3O_8$, when TiO_2 anatase phase is used in the starting mixture, especially when considering plasma spraying (Ref 6-8).

3.2 Transient Photocurrent-Time Profile of TiO_2 Electrode

Figure 6 shows a typical photocurrent-time profile of a TiO_2 electrode with hand-chopped light. An anodic photocurrent peak appears immediately after the light is turned on and then decreases continuously with time until a steady-state photocurrent is reached. When the light is turned off, the photocurrent decreases abruptly down to zero. The initial anodic photocurrent

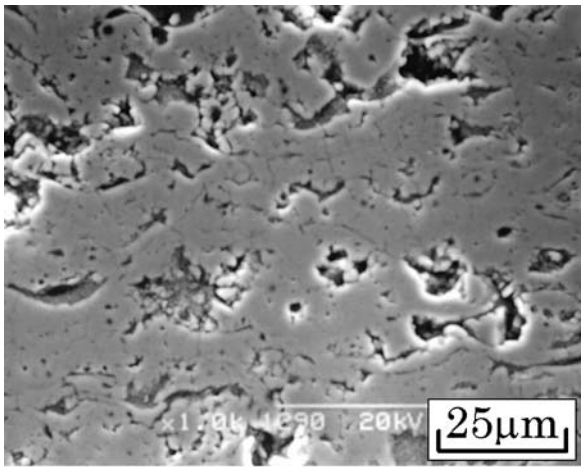

(a)

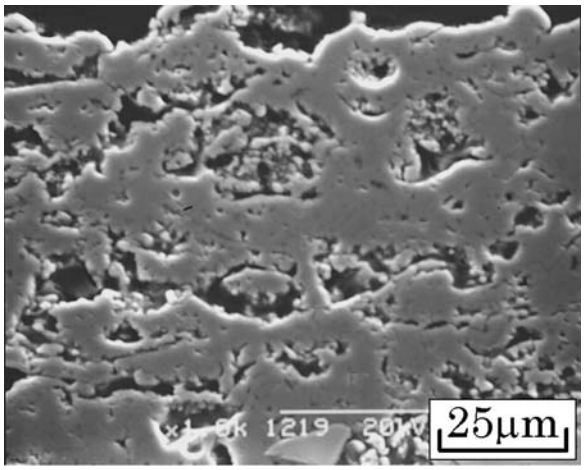

(b)

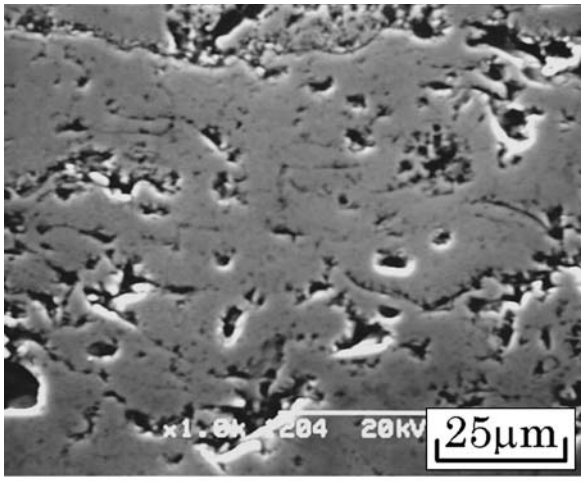

(c)

Fig. 2 Typical microstructures of the (a) plasma-sprayed TiO_2 electrode, (b) TiO_2-5%ZnO electrode, and (c) TiO_2-10%ZnO electrode

peak is due to instantaneous photo-induced electron transitions to the conduction band, as discussed by Liu et al. (Ref 9) and Salvador (Ref 10).

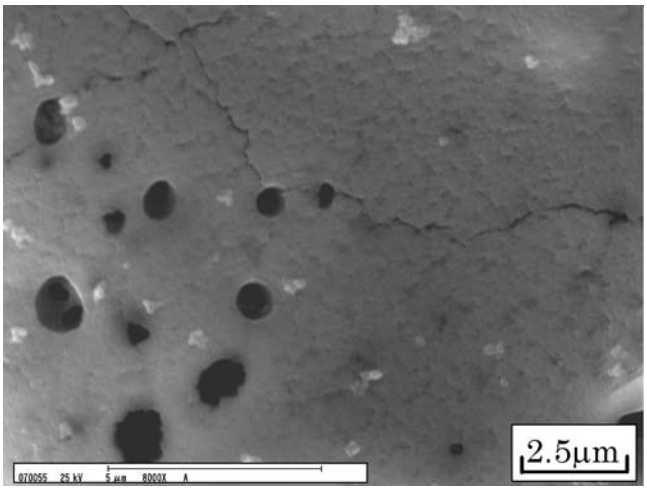

Fig. 3 Typical spherical pores of the plasma-sprayed TiO_2-ZnO electrode

3.3 Photoelectrochemical Characteristics of Sprayed TiO_2 and TiO_2-ZnO Electrodes

Figure 7 illustrates the photocurrent-potential curves of the TiO_2, TiO_2-5%ZnO, and TiO_2-10%ZnO electrodes sprayed under an arc current of 600 A. The photo-response characteristics of the sprayed electrodes are comparable to that of TiO_2 single crystal, but the breakdown voltage is about 0.5 V (versus that for the SCE), which is very similar to those of the plasma-sprayed electrodes prepared by Wang and Henager (Ref 3). The J_{SC} of the TiO_2-5%ZnO electrode is higher than that of the TiO_2 and TiO_2-10%ZnO electrodes prepared under the same spray parameters.

It has been reported that the electrode materials for photoelectrochemical conversion must exhibit optimal conductivity for the efficient movement and lowest recombination of excited hole-electron pairs. The variation of electrode resistivity can be understood in terms of the change in electron concentration induced by the possible defect reactions and the microstructure. Furthermore, because TiO_2 contains interstitial channels in the *c* direction, certain transition metals diffuse through these channels into lattices. The diffusing ions have been found to locate preferentially on either the substitutional or interstitial sites (Ref 5). The conductivity of the TiO_2 electrode decreases with the addition of ZnO. On the one hand, the increase of resistivity of the TiO_2-5%ZnO electrode can be explained by the substitution of the Ti site (0.68 Å) with the Zn site (0.74 Å). As a result, the electron concentration may be reduced, as expressed by:

$$ZnO + 2e' + \frac{1}{2}O_2 \rightarrow Zn_{Ti}^{\bullet\bullet} + 2O_o^{\times} \quad \text{(Eq 1)}$$

On the other hand, the increase of resistivity of the TiO_2-5%ZnO electrode results from the porous microstructure, as shown in Fig. 2, compared with the TiO_2 electrode. For the relative high resistivity, the recombination speed of hole-electron pairs of TiO_2-5%ZnO electrodes may decrease and then increase the J_{SC}. However, the far lower conductivity of the TiO_2-

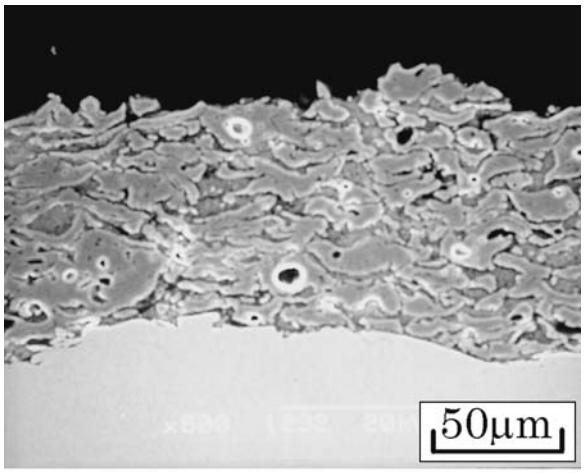

(a)

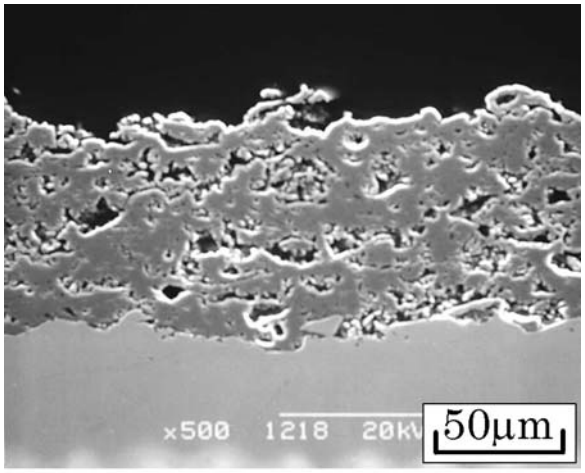

(b)

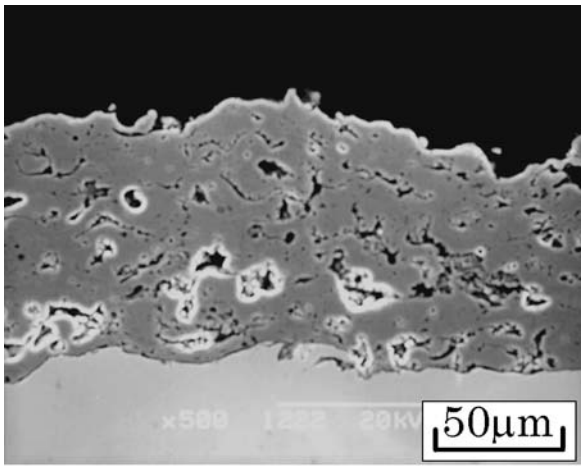

(c)

Fig. 4 Typical microstructures of plasma-sprayed TiO_2-5%ZnO electrodes under arc currents of (a) 400 A, (b) 600 A, and (c) 800 A

10%ZnO electrode may well increase ohmic loss and then lower the J_{SC}.

For the same powder, the J_{SC} of the electrodes prepared under an arc current of 600 A is higher than that under 400 or 800 A, as shown in Fig. 8, and it increases linearly with the light intensity, as shown in Fig. 9.

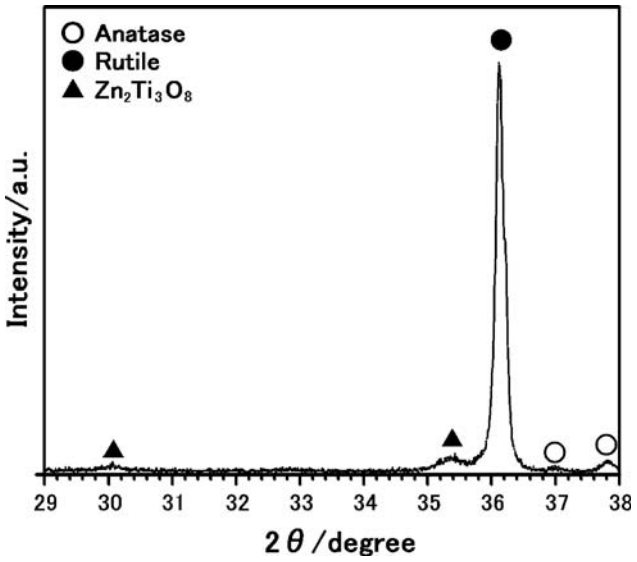

Fig. 5 Typical XRD pattern of a plasma-sprayed TiO_2-5%ZnO electrode

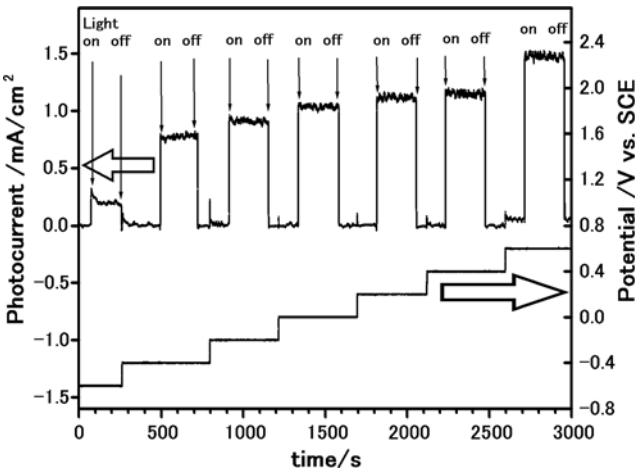

Fig. 6 Transient photocurrent-time profile of the TiO_2 electrode

3.4 Donor Concentration of Sprayed Electrodes

The semiconductor surface properties are of paramount importance, and their determination has received considerable effort. Because the donor concentration is one of the key parameters, it has been determined in this study from the quantum efficiency measurement according to the Gartner-Butler model (Ref 11). Generally, a low donor concentration will increase the J_{SC}.

According to the Gartner-Butler model, the quantum efficiency is expressed as:

$$J_{SC}^2 = \frac{2\varepsilon_R \varepsilon_0 e \alpha^2 I_0^2}{N_d}(V - V_{FB}) \quad \text{(Eq 2)}$$

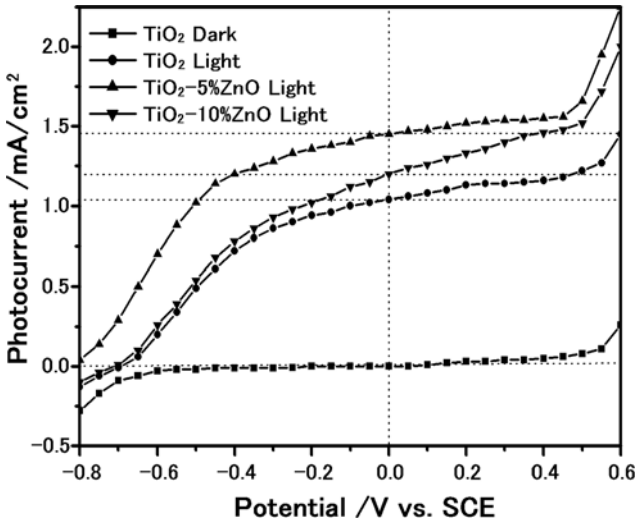

Fig. 7 Photocurrent-potential curves of the TiO_2, TiO_2-5%ZnO, and TiO_2-10%ZnO electrodes prepared under an arc current of 600 A

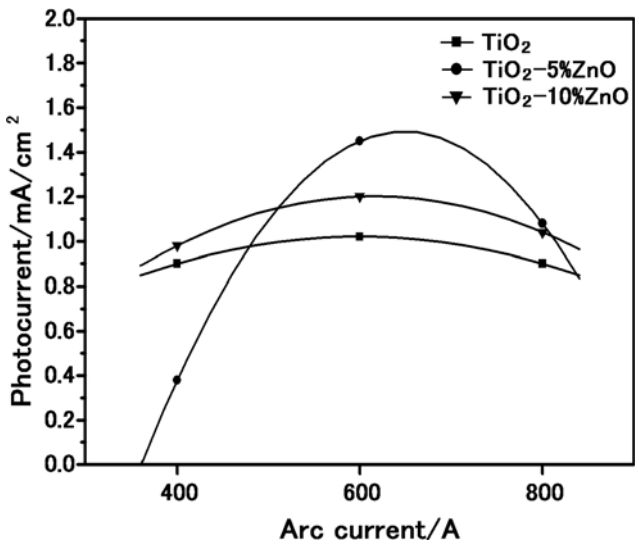

Fig. 8 Relationship between the photocurrent density and the arc current of the TiO_2, TiO_2-5%ZnO, and TiO_2-10%ZnO electrodes

where I_0 is the photo intensity (J/m^2), α is the optical absorption coefficient (m^{-1}), ε_0 is the permittivity of free space (F/m), ε_R is the relative dielectric constant, e is the elementary charge (C), V is the electrode potential (V), V_{FB} is the flatband potential (V), and N_d is the donor concentration (m^{-3}).

The donor concentration of the sprayed electrodes was calculated according to Eq 2, and the results are given in Fig. 10. The donor density of the electrode under an arc current of 600 A is lower than that under arc currents of 400 or 800 A for the same feedstock powder. The donor density of the TiO_2-5%ZnO electrode prepared under the arc current of 600 A is lower compared with those of the other electrodes. These results are in good relation with the J_{SC} shown in Fig. 8. It was previously mentioned that the J_{SC} increases linearly with the light intensity, which implies that Eq 2 is fulfilled, as also reported by Salvador (Ref 10).

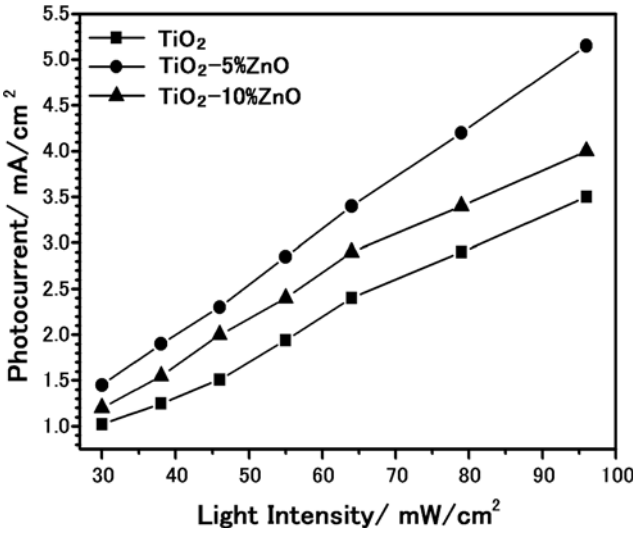

Fig. 9 Relationship between J_{SC} and light intensity

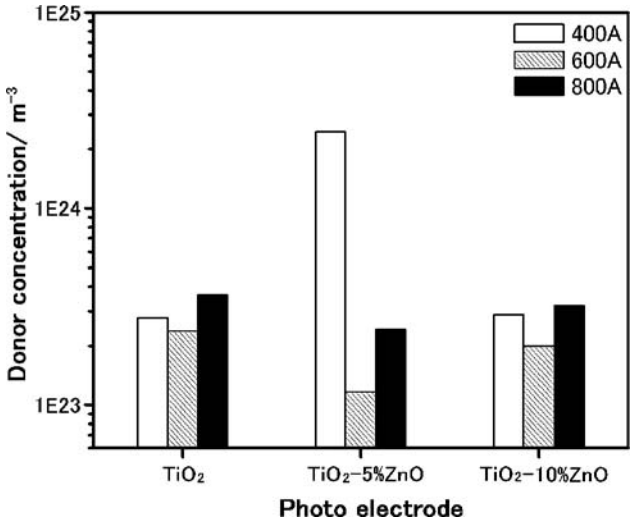

Fig. 10 Donor concentration of plasma-sprayed TiO_2, TiO_2-5%ZnO, and TiO_2-10%ZnO electrodes

4. Conclusions

In this study, the microstructure, composition, and photoelectrochemical performance of plasma-sprayed TiO_2, TiO_2-5%ZnO, and TiO_2-10%ZnO electrodes were systematically investigated. The porosity of the TiO_2-ZnO specimens increased with increasing amounts of ZnO. The TiO_2-ZnO electrodes prepared by plasma spraying consisted of anatase TiO_2, rutile TiO_2, and $Zn_2Ti_3O_8$ phases. The plasma-sprayed electrodes show photo-response characteristics, and the breakdown voltage is close to 0.5 V (versus that for the SCE). The maximum J_{SC} of the TiO_2-5%ZnO electrode is about 1.45 mA/cm^2, which is 0.4 mA/cm^2 higher than that of the TiO_2 electrodes under 30 mW/cm^2 xenon light irradiation. Furthermore, the linear dependence of the J_{SC} on light intensity is observed under a constant potential. Moreover, the donor concentration is in good relation with J_{SC}.

References

1. A. Fujishima and K. Honda, Electrochemical Photolysis of Water at a Semiconductor Electrode, *Nature,* Vol 238, 1972, p 37-38
2. A.L. Linsebigler, G.-Q Lu, and J.T. Yates Jr., Photocatalysis on TiO_2 Surfaces: Principles, Mechanisms, and Selected Results, *Chem. Rev.,* Vol 95, 1995, p 735-738
3. R. Wang and C.H. Henager Jr., Arc-Plasma-Sprayed Rutile Anodes for Photoelectrolysis of Water, *Electrochem. Soc*., Vol 126 (No.1), 1979, p 83-85
4. F.X. Ye and A. Ohmori, The Photocatalytic Activity and Photo-Absorption of Plasma Sprayed TiO_2-Fe_3O_4 Binary Oxide Coatings, *Surf. Coat. Technol.,* Vol 160, 2002, p 62-67
5. K.H. Yoon, J. Cho, and D.H. Kang, Physical and Photoelectrochemical Properties of the TiO_2-ZnO System, *Mater Res. Bull.,* Vol 34 (No. 9), 1999, p 1451-1461
6. A.I. Sheinkman, F.P. Sheinkman, I.P. Dobrovolskii, and S.A. Bolshakova, The Solid Solution of ZnO in Zinc Orthortitanate, *Inorg. Mater.,* Vol 13 (No. 3), 1977, p 383-386
7. A.I. Sheinkman, F.P. Sheinkman, I.P. Dobrovolskii, and S.A. Bolshakova, Phase Formation Sequence in the Reaction of Zinc Oxide with Titanium Dioxide, *Inorg. Mater.,* Vol 13 (No. 8), 1977, p 1171-1173
8. J. Yang and J.H. Swisher, The Phase Stability of $Zn_2Ti_3O_8$, *Mater. Charact.,* Vol 37 (No. 2-3), 1996, p 153-159
9. C. Liu, Y. Chen, and W. Li, Direct Observation of Elementary Steps in Charge Transfer Mediated by Surface States on TiO_2 Electrode Under Illumination, *Surf. Sci.,* Vol 163, 1985, p 383-390
10. P. Salvador, Subbandgap Photoresponse of n-TiO_2 Electrodes: Transient Photocurrent-Time Behavior, *Surf. Sci.,* Vol 192, 1987, p 36-46
11. S.E. Lindquist, B. Finnstrom, and L. Tegner, Photoelectrochemical Properties of Polycrystalline TiO_2 Thin Film Electrodes on Quartz Substrates, *J. Electrochem. Soc.,* Vol 130 (No. 2), 1983, p 351-358